

See discussions, stats, and author profiles for this publication at:
<https://www.researchgate.net/publication/318299863>

Investigation of mechanical, microstructural and thermal behavior of CoCrMo alloy manufactu....

Article · June 2017

DOI: 10.26678/ABCM.COBEP2017.COF2017-1286

CITATIONS

0

READS

197

3 authors, including:



Marcello Vertamatti Mergulhão

University of São Paulo

13 PUBLICATIONS **6** CITATIONS

[SEE PROFILE](#)



Mauricio Neves

Instituto de Pesquisas Energéticas e...

38 PUBLICATIONS **138** CITATIONS

[SEE PROFILE](#)

Some of the authors of this publication are also working on these related projects:



Fabricação de Ferramentas de Corte de Aços Rápidos ao Molibdênio Através de Técnicas de Metalurgia do Pó [View project](#)



Heat treatment in selective laser melting parts [View project](#)

INVESTIGATION OF MECHANICAL, MICROSTRUCTURAL AND THERMAL BEHAVIOR OF CoCrMo ALLOY MANUFACTURED BY SELECTIVE LASER MELTING AND CASTING TECHNIQUES

Marcello Vertamatti Mergulhão, marcellovertamatti@usp.br¹
Carlos Eduardo Podestá, eduardo@highbond.com.br^{1,2}
Maurício David Martins das Neves, mdneves@ipen.br¹

¹Instituto de Pesquisas Energéticas e Nucleares (IPEN/CNEN-SP) – CCTM, Av. Prof Lineu Prestes 2242, Cidade Universitária, Butantã, 05508-900, São Paulo, Brazil.

²High Bond Indústria de Ligas Metálicas Importação Exportação Ltda, Alameda Venus 661, Distrito Industrial American Park 13332-583, Indaiatuba, São Paulo, Brazil.

Abstract. A route of increasing development in additive manufacturing (3D printing) process using metal alloys is the selective laser melting (SLM). 3D building components is possible by laser power that completely melts the metal powder particles. SLM was applied in a biomaterial of CoCrMo alloy, to study the mechanical properties and microstructural characterization in comparison of the conventional technique – lost wax casting. The gas atomized powder was investigated by their physical (as apparent density, bulk density and flow rate) and chemical properties (X-ray fluorescence). Standard samples evaluated the mechanical properties as yield strength, elongation, elastic modulus, transverse rupture strength and the Vickers hardness. Microstructural characterization was performed using optical microscope (OM) and scanning electron microscope (SEM-EDS). Thermal analysis of CoCrMo alloy were investigated using thermomechanical analysis (TMA) and differential scanning calorimetry (DSC) techniques. The results of mechanical properties showed higher values in the SLM specimens compared with the obtained in the cast specimens. The micrographs revealed a typical morphology of consolidation process, characterized by selected layer used in the SLM technique and the dendrites arms in the casting technique. The thermal results confirm the phase's transitions of CoCrMo alloy.

Keywords: CoCrMo alloy, additive manufacturing, selective laser melting, lost-wax casting, biomaterial, powder metallurgy

1. INTRODUCTION

Cobalt-chromium alloys (Co-Cr) are widely used in various sectors of the industries, because of their high wear resistance and adequate corrosion resistance also being used in surface coating to increase performance components. The biocompatibility property this material is high and suitable being used in the manufacture of medical and dental prosthetics. (NARUSHIMA et al., 2013). In 1930, Co-Cr-Mo alloys (*Stellite*) processed by casting were used as dental alloys, and later adapted to attend orthopedic implants demand (NIINOMI; NARUSHIMA; NAKAI, 2015).

Advances have occurred in the area of processes using powder metallurgy techniques, making this technology competitive over other traditional manufacturing processes, such as casting, notably in health care. In this context, the additive manufacturing (AM) technologies, commonly referred by the term *Three Dimension Printing – 3DP*, stand out among the techniques to manufacture metals, ceramics and polymers. These technologies use digital imaging systems through CAD (Computer Aided Design) systems and promoting from the design to the prototypes (or even custom final geometry components) (GIBSON, 2005; GOUVEIA, 2009; VAN NOORT, 2012).

A route of increasing development in AM process using metal alloys is the selective laser melting (SLM). Components can be manufactured three-dimensional manner by means of a laser beam that completely melts particles of powder deposited layer by layer. The laser power on SLM machines can be up to 400 W with a laser focus diameter approximately to 100 µm (BREMEN; MEINERS; DIATLOV, 2012; MEINERS, 2012). SLM technique was promising since it allows the manufacture of customized components and high final physical properties compared to conventional techniques (casting and milling) (VAN NOORT, 2012). In these technology, it is possible to obtain several positive aspects, such as: reduction of waste, uniform microstructural characteristics, homogeneous mechanical properties, high dimensional accuracy and speed of manufacture with specific characteristics. It is described the possibility to obtaining components with approximately 100% of total density (CALIGNANO et al., 2017; YAP et al., 2015).

The aim of this study is to demonstrate the mechanical properties and microstructures of specimens manufactured by powder metallurgy techniques using the SLM, using the Co-Cr-Mo alloy in the form of particulate matter. Yet there is an important knowledge of performance properties, dimensional, mechanical and microstructural of this sintered

alloy compared to casting, as reported recently (MERGULHÃO; PODESTÁ; NEVES, 2015a, 2015b; PODESTÁ; MERGULHÃO; NEVES, 2015). Obtained properties must meet specific characteristics of health care performance.

2. MATERIAL AND METHODS

2.1. Material and manufacturing

The Co-Cr-Mo alloy was provided by the HighBond® (Indaiatuba, Brazil). To supply the powder used in the manufactured process by SLM technology, the alloy was gas atomized at H.C Starck® Company in the granulometric range of 15-45 µm. This study based on Co-Cr-Mo alloy with certification of ANVISA for use in health care. Several physical properties of gas-atomized powders were obtained such as flow time, apparent density, tap density of powders were performed according respectively to ASTM B212 (2013a), B213 (2013b) and ASTM B527 (2014). The particle size distribution was performed using a particular analyzer by laser scattering (Cilas - Model 1064). The particle format was analyzed by SEM - Philips XL30. The characterization by Helium pycnometry was performed in the Co-Cr-Mo powders used the Micromeritics machine - Model Accu PYC 1330 Pycnometer, located in the Nuclear Fuel Center (NFC/IPEN). The confirmation of chemical composition was performed in Co-Cr-Mo samples (powder, LC and SLM specimens) by fluorescence spectrometer X-ray energy dispersive (Shimadzu EDX-720 equipment), as a presented in the Tab. 1. in comparison with the standard ASTM F75 (2012a).

Table 1. Chemical composition (weight %) of Co-Cr-Mo samples (powder, LWC and SLM) and the standard reference ASTM F75 (2012a).

Elements (wt.%)	Co	Cr	Mo	Fe
Powder	63,93 ± 0,16	28,83 ± 0,19	7,07 ± 0,31	0,17 ± 0,01
LWC	66,38 ± 0,15	26,76 ± 0,21	6,68 ± 0,03	0,18 ± 0,08
SLM	65,38 ± 0,32	27,68 ± 0,13	6,61 ± 0,16	0,33 ± 0,06
ASTM F75	Balance	30,00 - 27,00 ± 0,30	7,00 - 5,00 ± 0,15	0,75 ± 0,03

The consolidation of SLM samples was carried out by SLM Solutions™ using a selective laser melting machine SLM®280HL with a single Ytterbium laser beam (30 µm - trick laser and 400W – laser power). The lost-wax casting (LWC) samples was performed according to ASTM F75 (2012a).

2.2. Mechanical tests

Mechanical characterization of consolidated samples by lost wax casting (LWC) and selective laser melting (SLM) techniques was held in standardized tensile samples (n=5) and bending samples (n=5), respectively according to ISO 22674 (2006) and ASTM B528 (2012b). The bending test were performed to obtained the transversal rupture strength (TRS). The TRS relates the applied load (P) and the distance between the supports (L), over the cross area of the sample (t, thickness and w, width), as show at the Eq. (1). The all mechanical tests were performed using a universal testing machine (Instron 3366) under a crosshead speed of 0.2 mm/min at room temperature.

$$TRS = \frac{3 \times P \times L}{2 \times t^2 \times w} \quad (1)$$

2.3. Microstructure characterization

The microstructural characterization and fracture analysis of consolidated Co-Cr-Mo was performed after tensile test. The tensile test specimens were sectioned the vertical direction and was prepared mechanical grinding (SiC paper # 1200) and final polishing (OP-S 0,02µm). The specimens were etching in solution: 100ml HCl and 2ml H₂O₂ (1-2 minutes at room temperature). The microstructural characterization was performed using an optical microscope - OM (Olympus - BX51M) and scanning electron microscope (SEM-EDS Philips XL30). To evaluate the internal porosity of cast and SLM sample were measured the pycnometer density in comparison by the theoretical density. The density by pycnometer Helium, considered only the internal porosity (excluding the open porosity) was measure using the Micromeritics equipment - Model Accu PYC 1330 Pycnometer.

2.4. Thermal characterization

The thermomechanical analysis (TMA) was performed to obtain the coefficient of thermal expansion (CET or $\alpha = 10^{-6} \text{ } ^\circ\text{C}^{-1}$) on samples consolidated by SLM and LWC of the Co-Cr-Mo alloy. In addition, the SLM samples were

analyzed in the parallel and transversal building direction (SLM 1 – parallel direction and SLM 2 – transversal direction). The routine of the TMA analysis remained similar to the DSC routine. However, the heating rate was from 10 °C/min until the temperature of 1300 °C. The equipment used in thermal analysis (DSC and TMA) was a Setaram - Setsys 16/18, with a thermocouple of Pt/Pt Rh 10% and a static atmosphere, constituted in argon (99.999%) was applied to exclude the sample oxidation.

The differential scanning calorimetry (DSC) analysis of the Co-Cr-Mo alloy powder was obtained from heating curve at rate of 10 °C/min until the temperature of 1300 °C. The purpose of the technique was to complement the thermal results of Co-Cr-Mo alloy and to correlate with the events occurred in TMA analysis. The sample port and the reference used in the analysis were composed of alumina (Al₂O₃) and the volume of Co-Cr-Mo powder was approximately 100 µL.

3. RESULTS AND DISCUSSION

3.1. Physical properties of materials

The characteristic format of the powder process fabrication by gas atomization is observed in the Fig. 1. The analysis in SEM show that the powders are spherical and presented satellites (appointed by arrows). The satellites can be formed in the surface particles during the cooling process of the spherical powder particles during gas atomization. It is noteworthy that the shape of the particle influences on packing properties, flow hate and compressibility, as well as reports on the powder metallurgy process (ASM INTERNACIONAL, 1998; GERMAN, 1994; GESSINGER, 1984). The cross-sectioned powder (Fig. 1b) shows the dendritic morphology with the primarily arms and ramifications, characterizing the rapid solidification of gas atomization process.

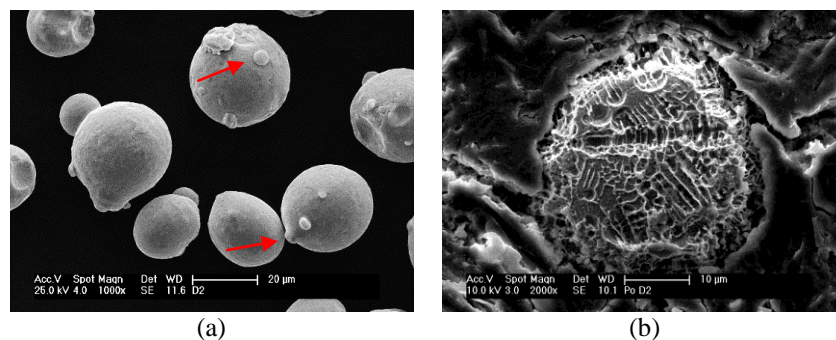


Figure 1. a) Micrographs of atomized powder (arrows indicate the satellites) and b) cross-section of powder after etch.

The powders for SLM manufacture technique have a mean diameter less than 50 microns to improve the physical properties like as flow time, apparent density and tap density (KURZYNOWSKI et al., 2012). The results of physical powder properties are summarized in the Tab. 2.

Table 2. Physical properties of Co-Cr-Mo powder used in the SLM manufacture.

Physical properties		Powder
Granulometric Distribution [µm]	Diameter of 10%	20.88
	Diameter of 50%	31.11
	Diameter of 90%	46.10
	Medium diameter	32.36
Flow Time [s/50g]		15.85 ± 0.11
Apparent Density [g/cm³]		4.51 ± 0.01
Tap Density [g/cm³]		5.26 ± 0.05
Relative Density [g/cm³]		8.38
Picnometry Density [g/cm³]		8.30 ± 0.11

According to Haan et al. (2015), Co-Cr-Mo powders with diameter D90 equal to 39 µm, the flowability was 18.60 s/50 g. The results were similar to those obtained for the present study, like as 15.86s/50g for D90 equal to 46.10 µm.

The result of tap density tends to be higher than the result of the apparent density, because of the particle's accommodation there is a decrease in the amount of voids between the particles (ASM INTERNACIONAL, 1998). As well as, the smaller the apparent density, the greater the percentage of increase the tap density.

It is possible to verify the presence of closed porosity that is not considered as a measure of the volume of helium, and consequently reduces the value of pycnometry density. The presence of internal porosity calculated in relation to theoretical density is approximately 1.3%.

3.2 Mechanical properties

The mechanical results of the tests for the LWC and SLM specimens are present in Table 1. Analyzing the values is possible to verify that in all properties the SLM technique results in higher properties than LWC technique. In according to standard ISO22674:06 the SLM and LWC specimens satisfied the type 5 criteria, in all mechanical properties, as shows in the Tab. 3 (ISO, 2006).

Table 1. Mechanical properties of CoCrMo specimens fabricated by LWC and SLM techniques.

Mechanical Properties	Consolidation technique		Standard ISO 22674: 06
	LWC	SLM	Type 5
Yield Strength (MPa)	646.7 ± 44,4	731.5 ± 40.3	500
Rupture Strength (MPa)	742.2 ± 106.8	1127.9 ± 0.1	-
Ultimate Tensile Strength (MPa)	771.7 ± 103.3	1136.9 ± 1.0	-
Elongation (%)	14.20 ± 2.8	13.7 ± 5.3	2
Elastic Modulus “E” (GPa)	223.42 ± 15.7	225.2 ± 14.4	150
Hardness Vickers (HV)	272.2 ± 20.5	334.8 ± 16.0	-
TRS (MPa)	1072.3 ± 4.6	2501.2 ± 9.7	-

The hardness of the SLM (334.8 HV) sample is higher in relation to FP (272.2 HV) sample. This increase in hardness is associated to the microstructure of refined grains obtained by the laser melting process. In addition, this occurrence is associated to the cooling rate of process. LWC process are characterized by the low and homogeneous cooling rate, in contrast to the SLM process are characterized by fast and small melting area. The high hardness in SLM sample can be associated to the presence of residual stresses in the sample from the SLM consolidation process (JABBARI et al., 2014; SHIOMI et al., 2004; SIMCHI; POHL, 2003).

The result of TRS samples (SLM = 2501.2 ± 9.7 MPa and LWC = 1072.3 ± 4.6 MPa) was satisfactory. However, the TRS test of LWC sample evidenced the ductility of the casting process by precision and was confirmed by the value of higher elongation. According to Mengucci et al. (2016), the TRS result for a similar composition of Co-Cr-Mo alloy, after the shoot-peened treatment followed by heat treatment for strain relief, result a TRS equal to 2700 ± 25 MPa. Therefore, the present results are acceptable comparing the data obtained with the study by Mengucci et al. (2016).

3.3. Microstructure analysis

Microstructural analysis by OM and SEM-EDS was carried out to understand the mechanical properties improved in the SLM specimens in relation to the casting process technique. Is possible to check the presence of porous in the both specimens (LWC – Fig. 2a and SLM – Fig. 2b), however at the casting sample the porous is smaller (microporous), but in large quantities. The porous in the laser melting are uneven (a little larger but in small quantity), occurred by problems of dispersing the powder in the bed layer and the presence of satellites/porous in the particulate. The microstructural analysis of LWC samples are describe a dendritic arms and ramifications with different solidification orientations (Fig. 2a) (JABBARI et al., 2014; YAMANAKA; MORI; CHIBA, 2015; ZANGENEH; LASHGARI; ROSHANI, 2012).

SLM specimens shows a characteristic morphology (weld-like structure) of laser bean melting, and is possible to check the layers formed during the manufacture process (Fig. 2b). In the vertical section of SLM sample is observe the building direction of specimen (indicated by blue arrow). In addition, the SLM sample is characterized by the overlapping of each layer and the morphology formation by the action of the laser beam like as the weld pool. The microstructure observed in the samples is in agreement with that described by authors in the literature (HAAN et al., 2015; XIN et al., 2012; RIVERA et al., 2011).

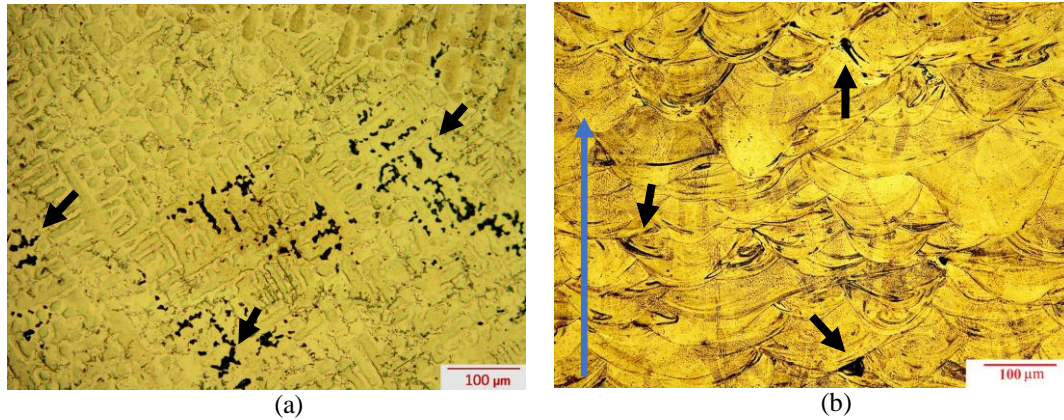


Figure 2. OM images of CoCrMo specimens after chemical etch (black arrows indicate the porous): a) as cast sample and b) as SLM (blue arrow indicate building direction).

LWC and SLM specimens were analyzed by SEM-EDS, as shown in Fig. 3 and Fig. 4, with backscattering electron (BSE) images after chemical etching. Fig. 3 is possible to identify the cast specimen with a second phase (white area) in the matrix. The semi quantitative analysis with the EDS and the respectively spectrums (Fig. 3c and 3d) shows that the composition of white area (point 1) is rich in Mo element and the matrix (point 2) are composed by Co-Cr elements, with a small percentage of Mo. The phase (point 1) shows the confirmation of carbide ($M_{23}C_6$) presence, rich in chromium and molybdenum (JABBARI et al., 2014; YAMANAKA; MORI; CHIBA, 2015; ZANGENEH; LASHGARI; ROSHANI, 2012).

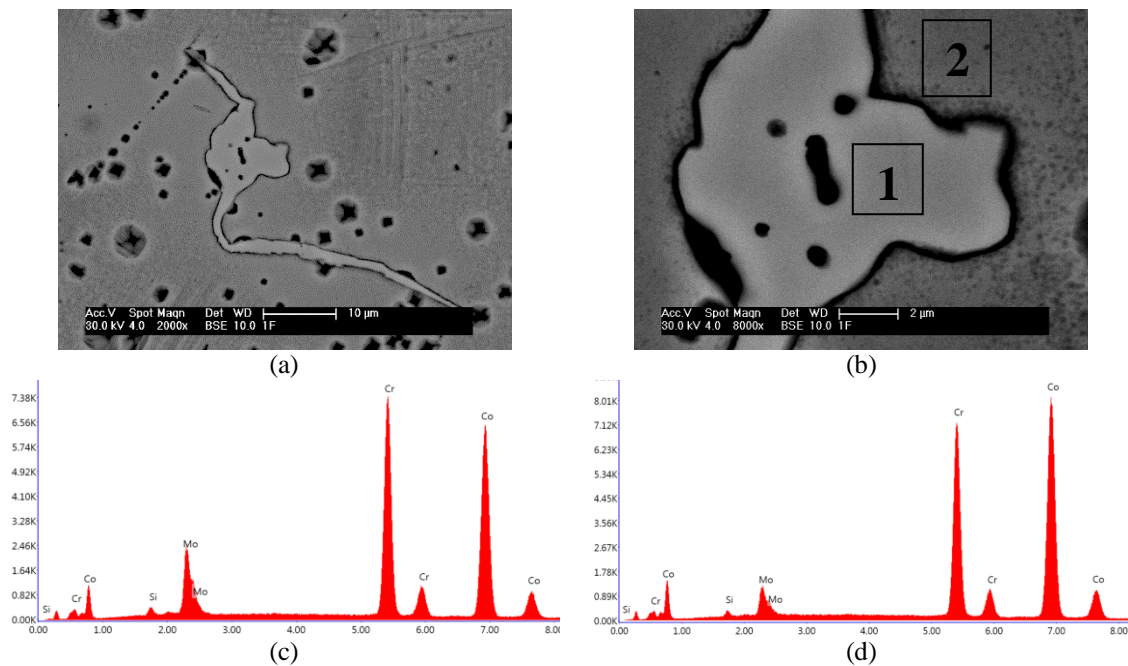


Figure 3. a) SEM image of LWC samples, b) high magnification of sample with points of EDS analyses, c) spot 1 and d) spot 2 spectrums of EDS analyses.

SLM specimen, as shown in Fig. 4, presented a microstructure formed with small grains characterizing the rapid solidification during the SLM manufacturing process. The semi quantitative analysis in the fine grains shows that has not different elements compositions. SLM specimen presents a homogeneous matrix with CoCrMo elements (HAAN et al., 2015). The morphology formation of the laser melting sample was also observed after electrolytic attack (BARUCCA et al., 2015; HAAN et al., 2015; RIVERA et al., 2011; XIN et al., 2012). As well as possible confirm that the fine grains are oriented in direction of the laser scanning. This characteristic microstructure of laser melting technique allows achieve better mechanical properties than the cast technique.

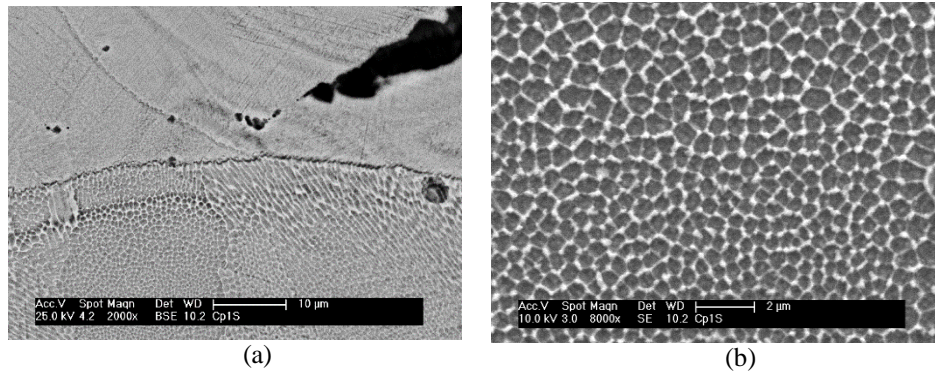


Figure 4. SEM images of SLM samples (a) BSE image and (b) SE image.

3.4. Thermal analysis

The heating curves obtained from TMA and DSC analysis in the form of powder, LWC and SLM sample are presented in Fig. 5. From the TMA curves is possible observe that the CET for the consolidated samples has a different behavior between the processes of Co-Cr-Mo alloy. As it is possible to verify the CET of samples SLM 1, SLM 2 and F at the temperature of 500 °C is respectively 15,0 / 19,5 / 22,0 $\cdot 10^{-6}$ °C⁻¹. At the temperature of 600 °C the coefficient value decreases to the values of 12.5 / 14.5 / 18.5 $\cdot 10^{-6}$ °C⁻¹. As reported in literature (ASM INTERNACIONAL, 2000; CRAIG, 2012; SANTOS, 2012), the metal alloys for use as dental materials must have a CET of approximately 15.5 $\cdot 10^{-6}$ °C⁻¹, providing a good adjustment due to contraction and expansion during heating, thus avoiding the possibility of voids or cracks occurring during the firing process.

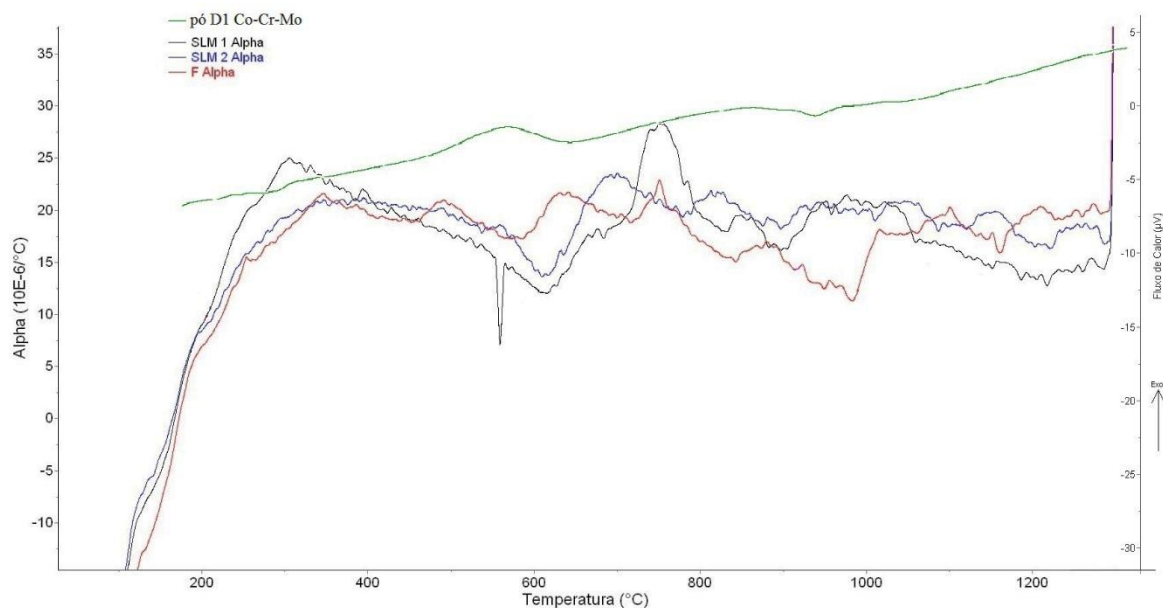


Figure 5. Thermal curves of consolidated Co-Cr-Mo samples (powder, LWC and SLM): DSC analysis of powder sample (green curve) and TMA analysis of LWC sample (red curve), SLM 1 – building direction (black curve) and SLM 2 – transversal of building direction (blue curve).

To investigate and confirm the thermal events presents in the Co-Cr-Mo alloy the heating curves (DSC and TMA analyzes) were juxtaposed. As can be seen in the DSC and TMA curves are similarity in the temperatures ranges of events. Is possible observed two events, the first event occurs in the range of 514 to 614 °C and the second event at 923 to 961 °C. In the case of the LWC sample (red curve – F), it is possible to verify that the events occur in a higher temperature in relation to the samples processed by SLM. This occurrence is associated to the samples microstructure of analysis performed. The powder sample (green curve - DSC analysis) has a dendritic microstructure, as the same of the LWC sample (red curve – F). TMA curves of SLM samples (SLM 1 – black curve and SLM 2 – blue curve) shows more evident peaks, but the transition of these events set at increased temperatures. So, this occurrence is provided

because the laser melting process provide a refine microstructure, difficulty the phase transitions and necessity superior temperatures to occur the events. In a similar analysis to the present study, Facchini (2010) shows the DSC and TMA analysis curve (heating rate of 20 °C/min) performed in an ASTM F75 composition alloy and processed by electron beam fusion (EBM). And is possible to relate the DSC analysis, which: the first peak (565-900 °C) is associated with the transition from the FCC (α Co) phase to the HCP (ϵ Co) phase, and the second peak (900-1000 °C) reduces the HCP phase (ϵ Co) and reappearance of the FCC phase (α Co).

4. CONCLUSIONS

The particles in the study produced by gas atomization showed spherical particle geometry with satellites and internal porosity. The microstructural characterization of the LWC samples showed formation of carbide rich in molybdenum and chromium elements. The selective laser melting allowed obtaining samples with improved chemical homogeneity over the molten sample, and with lower presence of porosity. The SLM technique allowed obtaining samples with superior mechanical properties of the precision casting technique. The thermal analyzes showed the present phase transitions of Co-Cr-Mo alloy, as well as being possible to correlate them (TMA to DSC curves). The coefficient of thermal expansion (CET) resulted for both processes a pertinent value to alloys used in dental materials. The processing using laser melting proved superior to casting processing technique, allowing the use of this technique in the manufacturing area of prosthetics and dental implants.

5. ACKNOWLEDGEMENTS

This study was financially support by CNPq. The authors also thank to Ms. Amed Belaid and SLM® Solution for tensile and bending SLM specimens.

6. REFERENCES

- ASM INTERNACIONAL. **Powder Metal Technologies and Applications**. 9. ed. [s.l.] ASM Internacional, 1998. v. 7
- ASM INTERNACIONAL. **ASM Specialty Handbook: Nickel, Cobalt, and Their Alloys**. 1. ed. [s.l.] ASM Internacional, 2000.
- ASTM INTERNATIONAL. **F75-12 - Standard Specification for Cobalt-28 Chromium-6 Molybdenum Alloy Castings and Casting Alloy for Surgical Implants**. Pensilvânia: ASTM, 2012a.
- ASTM INTERNATIONAL. **B528-12 - Standard Test Method for Transverse Rupture Strength of Powder Metallurgy (PM) Specimens**. Pensilvânia: ASTM, 2012b.
- ASTM INTERNATIONAL. **B212-13 - Standard Test Method for Apparent Density of Free-Flowing Metal Powders Using the Hall Flowmeter Funnel**. Pensilvânia: ASTM, 2013a.
- ASTM INTERNATIONAL. **B213-13 - Standard Test Methods for Flow Rate of Metal Powders Using the Hall Flowmeter Funnel**. Pensilvânia: ASTM, 2013b.
- ASTM INTERNATIONAL. **B527-14 - Standard Test Method for Determination of Tap Density of Metal Powders and Compounds**. Pensilvânia: ASTM, 2014.
- Barucca, G. et al. Structural characterization of biomedical Co–Cr–Mo components produced by direct metal laser sintering. **Materials Science and Engineering: C**, v. 48, p. 263–269, mar. 2015.
- Bremen, S.; Meiners, W.; Diatlov, A. Selective Laser Melting: A manufacturing technology for the future? **Laser Technik Journal**, v. 9, n. 2, p. 33–38, abr. 2012.
- Calignano, F. et al. Overview on Additive Manufacturing Technologies. **Proceedings of the IEEE**, p. 1–20, 2017.
- Craig, R. G. **Craig's Restorative Dental Materials**. 13. ed. [s.l.] Elsevier/ Mosby, 2012.
- Facchini, L. **Microstructure and mechanical properties of biomedical alloys produced by Rapid Manufacturing techniques**. Doutorado—Italy: University of Trento, 2010.
- German, R. M. **Powder Metallurgy Science**. 2. ed. Princeton: Metal Powder Industry Federation, 1994.
- Gessinger, G. H. **Powder Metallurgy of Superalloys**. Baden, Switzerland: Butterworth & Co., 1984.
- Gibson, I. **Advanced Manufacturing Technology for Medical Applications: Reverse Engineering, Software Conversion and Rapid Prototyping**. [s.l.] Wiley, 2005.
- Gouveia, M. F. **Aplicação da Prototipagem Rápida no Planejamento de Cirurgias Craniofaciais**. Doutorado—Campinas: Unicamp, 2009.
- Haan, J. et al. Effect of subsequent Hot Isostatic Pressing on mechanical properties of ASTM F75 alloy produced by Selective Laser Melting. **Powder Metallurgy**, v. 58, n. 3, p. 161–165, jul. 2015.
- ISO. **22674-06 - Dentistry - Metallic materials for fixed and removable restorations and appliances**. Geneva: 2006.
- Jabbari, Y. S. A. et al. Metallurgical and interfacial characterization of PFM Co–Cr dental alloys fabricated via casting, milling or selective laser melting. **Dental Materials**, v. 30, n. 4, p. e79–e88, 1 abr. 2014.

- Kurzynowski, T. et al. **Parameters in selective laser melting for processing metallic powders**. Disponível em: <<http://proceedings.spiedigitallibrary.org/proceeding.aspx?doi=10.1117/12.907292>>. Acesso em: 3 ago. 2016
- Mengucci, P. et al. Effects of thermal treatments on microstructure and mechanical properties of a Co–Cr–Mo–W biomedical alloy produced by laser sintering. **Journal of the Mechanical Behavior of Biomedical Materials**, v. 60, p. 106–117, jul. 2016.
- MEINERS, W. Selective Laser Melting: Generative Fertigung für die Produktion der Zukunft Optische Technologien in der Produktionstechnik. 2012.
- Mergulhão, M. V.; Podestá, C. E.; Neves, M. D. M. Das. **Evaluation of Mechanical Properties and Microstructural Characterization of ASTM F75 CoCrMoFe Alloy Obtained by Selective Laser Sintering (SLS) and Casting Techniques**. . In: PTECH 2015 - TENTH INTERNATIONAL LATIN AMERICAN CONFERENCE ON POWDER TECHNOLOGY. Mangaratiba - RJ: 2015a
- Mergulhão, M. V.; Podestá, C. E.; Neves, M. D. M. Das. **Mechanical Properties and Microstructural Characterization of Cobalt-Chromium (CoCr) Sintered Obtained by Casting and Selective Laser Sintering (SLS)**. . In: PTECH 2015 - TENTH INTERNATIONAL LATIN AMERICAN CONFERENCE ON POWDER TECHNOLOGY. Mangaratiba - RJ: 2015b
- Narushima, T. et al. Precipitates in Biomedical Co-Cr alloys. **Precipitates in Biomedical Co-Cr alloys**, v. 65, n. 4, p. 489–504, 2013.
- Niinomi, M.; Narushima, T.; Nakai, M. **Advances in Metallic Biomaterials**. Berlin, Heidelberg: Springer Berlin Heidelberg, 2015. v. 3
- Podestá, C. E.; Mergulhão, M. V.; Neves, M. D. M. Das. **Comparative Study of Mechanical Properties Between Casting and Selective Laser Sintering (SLS) in Cobalt-Chromium Alloys**. . In: POWDERMET2015, THE INTERNATIONAL CONFERENCE ON POWDER METALLURGY & PARTICULATE MATERIALS. San Diego: 2015
- Rivera, S. et al. DEVELOPMENT OF DENSE AND CELLULAR SOLIDS IN CRCOMO ALLOY FOR ORTHOPAEDIC APPLICATIONS. **Procedia Engineering**, v. 10, p. 2979–2987, 2011.
- Santos, L. A. **Processamento e caracterização da liga 66Co-28Cr-6Mo (% peso) para implantes**. Dissertação de Mestrado—Lorena: Universidade de São Paulo, 2012.
- Shiomi, M. et al. Residual Stress within Metallic Model Made by Selective Laser Melting Process. **CIRP Annals - Manufacturing Technology**, v. 53, n. 1, p. 195–198, 1 jan. 2004.
- Simchi, A.; Pohl, H. Effects of laser sintering processing parameters on the microstructure and densification of iron powder. **Materials Science and Engineering: A**, v. 359, n. 1–2, p. 119–128, Outubro 2003.
- Van Noort, R. The future of dental devices is digital. **Dental Materials: Official Publication of the Academy of Dental Materials**, v. 28, n. 1, p. 3–12, jan. 2012.
- Xin, X. Z. et al. In vitro biocompatibility of Co–Cr alloy fabricated by selective laser melting or traditional casting techniques. **Materials Letters**, v. 88, p. 101–103, Dezembro 2012.
- Yamanaka, K.; Mori, M.; Chiba, A. Assessment of precipitation behavior in dental castings of a Co–Cr–Mo alloy. **Journal of the Mechanical Behavior of Biomedical Materials**, v. 50, p. 268–276, Outubro 2015.
- YAP, C. Y. et al. Review of selective laser melting: Materials and applications. **Applied Physics Reviews**, v. 2, n. 4, p. 041101, dez. 2015.
- Zangeneh, S.; Lashgari, H. R.; Roshani, A. Microstructure and tribological characteristics of aged Co–28Cr–5Mo–0.3C alloy. **Materials & Design**, v. 37, p. 292–303, maio 2012.

7. RESPONSIBILITY NOTICE

The author(s) is (are) the only responsible for the printed material included in this paper.